Notes on Power System Voltage Stability

By S. Chakrabarti, Dept. of EE, IIT, Kanpur

1. Power System Voltage Stability

At any point of time, a power system operating condition should be stable, meeting various operational criteria, and it should also be secure in the event of any credible contingency. Present day power systems are being operated closer to their stability limits due to economic and environmental constraints. Maintaining a stable and secure operation of a power system is therefore a very important and challenging issue. Voltage instability has been given much attention by power system researchers and planners in recent years, and is being regarded as one of the major sources of power system insecurity. Voltage instability phenomena are the ones in which the receiving end voltage decreases well below its normal value and does not come back even after setting restoring mechanisms such as VAR compensators, or continues to oscillate for lack of damping against the disturbances. Voltage collapse is the process by which the voltage falls to a low, unacceptable value as a result of an avalanche of events accompanying voltage instability [1]. Once associated with weak systems and long lines, voltage problems are now also a source of concern in highly developed networks as a result of heavier loading.

The main factors causing voltage instability in a power system are now well explored and understood [1-13]. A brief introduction to the basic concepts of voltage stability and some of the conventional methods of voltage stability analysis are presented in this chapter. Simulation results on test power systems are presented to illustrate the problem of voltage stability and the conventional methods to analyze the problem. Limitations of conventional methods of voltage stability analysis are pointed out and the scope of the use of Artificial Neural Networks as a better alternative is discussed.

2. Classification of voltage stability

The time span of a disturbance in a power system, causing a potential voltage instability problem, can be classified into short-term and long-term. The corresponding voltage stability dynamics is called short-term and long-term dynamics respectively [2-5]. Automatic voltage regulators, excitation systems, turbine and governor dynamics fall in this short-term or 'transient' time scale, which is typically a few seconds. Induction motors, electronically operated loads and HVDC interconnections also fall in this category. If the system is stable, short-term disturbance dies out and the system enters a slow long-term dynamics. Components operating in the long-term time frame are transformer tap changers, limiters, boilers etc. Typically, this time frame is for a few minutes to tens of minutes. A voltage stability problem in the long-term time frame is mainly due to the large electrical distance between the generator and the load, and thus depends on the detailed topology of the power system.

Figure 1.1 shows the components and controls that may affect the voltage stability of a power system, along with their time frame of operation [1]. Examples of short-term or transient voltage instability can be found in the instability caused by rotor angle imbalance or loss of synchronism. Recent studies have shown that the integration of highly stressed HVDC links degrades the transient voltage stability of the system [1].

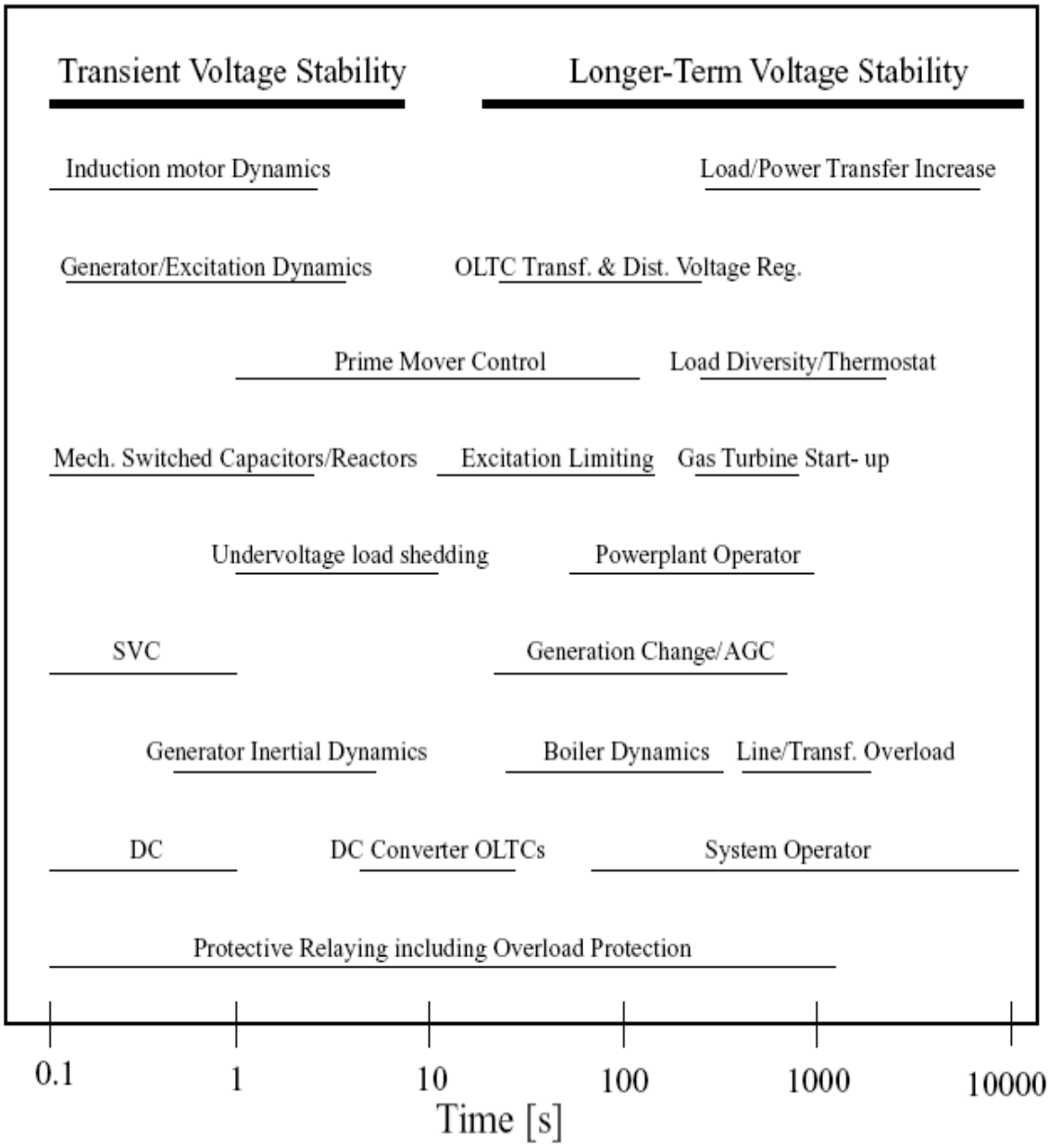

Figure 1.1: Time responses of different controls and components to voltage stability [1]

There is not much scope for operator intervention in transient voltage instability. The transmission system operator (TSO) mainly relies on automatic emergency actions to avoid incumbent voltage instability. The automatic corrective actions are taken through protective devices to preserve operation of largest possible part of the power system by isolating the unstable part [6].

Long-term voltage instability (or mid-term or post-transient, as it is sometimes called) problems can occur in heavily loaded systems where the electrical distance is large between the generator and the load. The instability may be triggered by high power imports from remote generating stations, a sudden large disturbance, or a large load buildup (such as morning or afternoon pickup). Operator intervention may be possible if the time scale is long enough. Timely application of reactive power compensation or load shedding may prevent this type of voltage instability.

From the point of view of techniques used to analyze the voltage stability, it is often useful to categorize the problem into small-disturbance and large-disturbance voltage stability [2]. Small disturbance or steady state voltage stability deals with the situation when the system is subjected to a small perturbation, such that the system can be analyzed by linearizing around the pre-disturbance operating point. Steady state stability analysis is helpful in getting a qualitative picture of the system, i.e., how stressed the system is, or how close the system is, to the point of instability. Examples of steady state stability can be found in power systems experiencing gradual change in load.

Large-disturbance stability deals with larger disturbances such as loss of generation, loss of line etc. To analyze the large-disturbance stability, one has to capture the system dynamics for the whole time frame of the disturbance. A suitable model of the system has to be assumed and a detailed dynamic analysis has to be carried out in order to get a clear picture of the stability.

3. Voltage stability of a simple 2-bus system

The basic concept of voltage stability can be explained with a simple 2-bus system shown in Figure 1.2. The load is of constant power type. Real power transfer from bus 1 to 2 is given by [4],

$$P = \frac{EV}{X}\sin\delta \tag{1.1}$$

Reactive power transfer from bus 1 to 2 is given by,

$$Q = -\frac{V^2}{X} + \frac{EV}{X}\cos\delta \tag{1.2}$$

where, $\mathbf{E} = E\angle\delta$ is the voltage at bus 1,

$\mathbf{V} = V\angle 0$ is the voltage at bus 2,

X= impedance of the line (neglecting resistance),

δ = power angle.

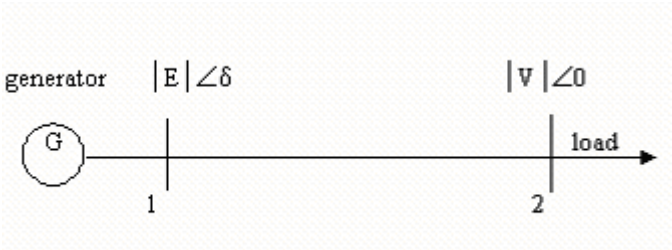

Figure 1.2: 2-bus test system

Normalizing the terms in (1.1) and (1.2) with $v = V/E$, $p = P.X/E^2$ and $q = Q.X/E^2$, one obtains,

$$p = v \sin \delta \tag{1.3}$$

$$q = -v^2 + v \cos \delta \tag{1.4}$$

Squaring the two equations above and rearranging,

$$v^2 (\sin^2 \delta + \cos^2 \delta) = p^2 + (q + v^2)^2$$

or,
$$v^4 + v^2 (2q - 1) + (p^2 + q^2) = 0 \tag{1.5}$$

Positive real solutions of v from (1.5) are given by,

$$v = \sqrt{\frac{1}{2} - q \pm \sqrt{\frac{1}{4} - p^2 - q}} \tag{1.6}$$

A plot of v on the p-q-v plane is shown in Figure 1.3 [4]. Corresponding to each point (p,q), there are two solutions for voltage, one is the high voltage or stable solution, which is the actual voltage at the bus, and the other one is the low voltage or unstable solution. The equator, along which the two solutions of v are equal, represents maximum power points. Starting from any operating point on the upper part of the surface, an increase in p or q or both brings the system closer to the maximum power point. An increase in p or q beyond the maximum power point makes the voltage unstable.

The preceding discussion illustrates voltage instability caused by an increase in system loading. In a real power system, voltage instability is caused by a combination of many additional factors which includes the transmission capability of the network, generator reactive power and voltage control limits, voltage sensitivity of the load, characteristics of reactive compensation devices, action of voltage control devices such as transformer under load tap changers (ULTCs) etc.

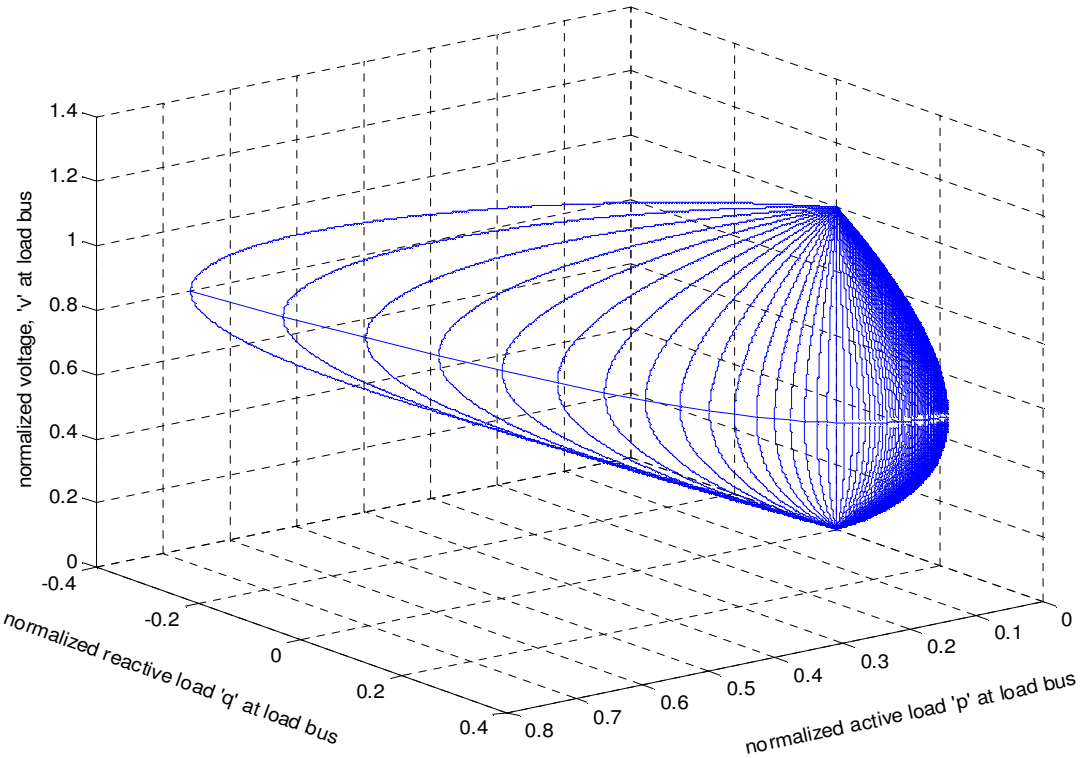

Figure 1.3: Variation of bus voltage with active and reactive loading for the 2-bus test system

4. Tools for voltage stability analysis

Different methods exist in the literature for carrying out a steady state voltage stability analysis. The conventional methods can be broadly classified into the following types.

1. P-V curve method.
2. V-Q curve method and reactive power reserve.
3. Methods based on singularity of power flow Jacobian matrix at the point of voltage collapse.
4. Continuation power flow method.

4.1 P-V curve method

This is one of the widely used methods of voltage stability analysis. This gives the available amount of active power margin before the point of voltage instability. For radial systems, the voltage of the critical bus is monitored against the changes in real power consumption. For large meshed networks, P can be the total active load in the load area and V can be the voltage of the critical or representative bus. Real power transfer through a transmission interface or interconnection also can be studied by this method.

For a simple two-bus system as shown in Figure 1.2, equation (1.6) gives real solutions of v^2, provided $(1 - 4q - 4p^2) \geq 0$.

Assuming a constant power factor load such that q/p = k (constant), the inequality can be expressed as,

$$p \leq \frac{1}{2}((1+k^2)^{1/2} - k) \tag{1.7}$$

For values of 'p' satisfying (1.7), there are two solutions of v as follows:

$$v_1 = (1/2 - pk + (1/4 - pk - p^2)^{1/2})^{1/2} \tag{1.8}$$

and

$$v_2 = (1/2 - pk - (1/4 - pk - p^2)^{1/2})^{1/2} \tag{1.9}$$

For real values of v_1 and v_2, the terms under the square roots should be positive.

Hence, $(1/2 - pk - (1/4 - pk - p^2)^{1/2}) \geq 0$

or, $p^2(k^2 + 1) \geq 0$ (1.10)

which is always true.

Hence (1.7) is the inequality that determines the maximum value of p.

Thus, representing the load as a constant power factor type, with a suitably chosen power factor, the active power margin can be computed from (1.7). For different values of load power factors, i.e., for different corresponding values of 'k', the normalized values of load active power are shown in Figure 1.4.

In practice, it is possible to find the Thevenin equivalent of any system with respect to the bus under consideration. It is to be noted that the generations are rescheduled at each step of change of the load. Some of the generators may hit the reactive power limit. The network topology may keep changing with respect to the critical bus, with change in the loading, thereby reducing the accuracy of the method. This method works well in the case of an infinite bus and isolated load scenario.

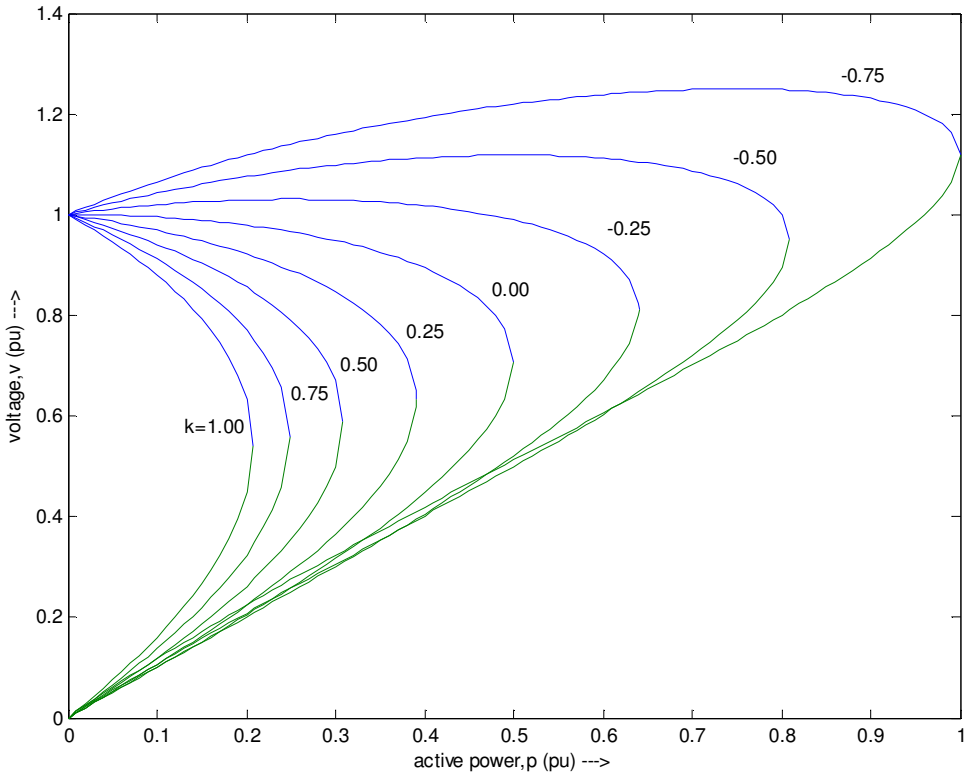

Figure 1.4: Normalized P-V curves for the 2-bus test system

4.2 V-Q curve method and reactive power reserve

The V-Q curve method is one of the most popular ways to investigate voltage instability problems in power systems during the post transient period [1, 4, 5]. Unlike the P-V curve method, it doesn't require the system to be represented as two-bus equivalent. Voltage at a test bus or critical bus is plotted against reactive power at that bus. A fictitious synchronous generator with zero active power and no reactive power limit is connected to the test bus. The power-flow program is run for a range of specified voltages with the test bus treated as the generator bus. Reactive power at the bus is noted from the power flow solutions and plotted against the specified voltage. The operating point corresponding to zero reactive power represents the condition when the fictitious reactive power source is removed from the test bus.

Voltage security of a bus is closely related to the available reactive power reserve, which can be easily found from the V-Q curve of the bus under consideration. The reactive power margin is the MVAR distance between the operating point and either the nose point of the V-Q curve or the point where capacitor characteristics at the bus are tangent to the V-Q curve [1]. Stiffness of the bus can be qualitatively evaluated from the slope of the right portion of the V-Q curve. The greater the slope is, the less stiff is the bus, and therefore the more vulnerable to voltage collapse it is. Weak busses in the system can be determined from the slope of V-Q curve.

For the simple two-bus system shown in Figure 1.2, equations of V-Q curves for constant power loads can be derived as follows. From (1.3) the power angle δ is computed for specified active power and used in (1.4). For a range of values of voltage and different active power levels, normalized V-Q curves are shown in Figure 1.5. The critical point or nose point of the characteristics corresponds to the

voltage where dQ/dV becomes zero. If the minimum point of the V-Q curve is above the horizontal axis, then the system is reactive power deficient. Additional reactive power sources are needed to prevent a voltage collapse. In Figure 1.5, curves for p=1.00 and p=0.75 signify reactive power deficient busses. Busses having V-Q curves below the horizontal axis have a positive reactive power margin. The system may still be called reactive power deficient, depending on the desired margin.

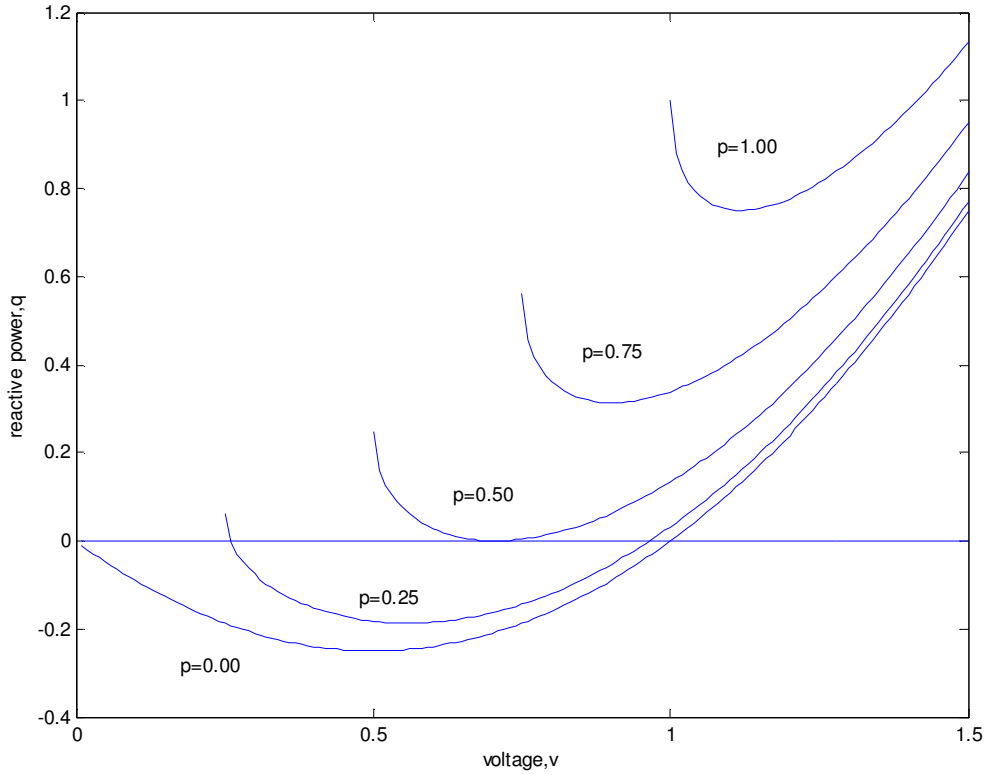

Figure 1.5: Normalized V-Q curves for the 2-bus test system

4.3 Method based on singularity of power-flow Jacobian matrix at the point of voltage collapse

A number of methods have been proposed in the literature that uses the fact that the power flow Jacobian matrix becomes singular at the point of voltage collapse. Modal analysis [2, 5, 14] of the Jacobian matrix is one of the most popular methods.

4.3.1 Modal analysis

For a (n x n) square matrix **A**, left and right eigenvectors are defined as follows:

$$\mathbf{A}\mathbf{x} = \lambda\mathbf{x} \tag{1.11}$$

$$\mathbf{y}\mathrm{A} = \lambda\mathbf{y} \tag{1.12}$$

where λ = eigenvalue of the matrix **A, x** (n x 1) = right eigenvector, **y** (1 x n) = left eigenvector.

The characteristic equation of both (1.11) and (1.12) is,

$$\det(\mathbf{A}-\lambda\mathbf{I}) = 0 \tag{1.13}$$

The solution of (1.13), i.e., $\lambda_1,\lambda_2,\ldots,\lambda_n$ are the eigenvalues of **A**. For different eigenvalues λ_i, i = 1,…,n, the right and left eigenvectors are defined as, $\mathbf{x}_i$, i = 1,…,n and $\mathbf{y}_i$, i = 1,…,n. In matrix form, the right eigenvector matrix, $\mathbf{X} = [\mathbf{x}_1, \mathbf{x}_2,\ldots, \mathbf{x}_n]$ and the left eigenvector matrix, $\mathbf{Y} = [\mathbf{y}_1^T,\mathbf{y}_2^T,\ldots,\mathbf{y}_n^T]^T$.
It can be shown that, $\mathbf{x}_j$ and $\mathbf{y}_i$ are orthogonal, such that,

$$\begin{aligned} \mathbf{y}_i.\mathbf{x}_j &= 0, \quad \forall\, i \neq j \\ &\neq 0, \quad \forall\, i = j \end{aligned}$$

In practice, eigenvectors are normalized so that $\mathbf{y}_i.\mathbf{x}_i = 1$, $\forall$ i = 1,…,n.

Hence, $\mathbf{Y}.\mathbf{X} = \mathbf{I}$, or, $\mathbf{Y} = \mathbf{X}^{-1}$ (1.14)

Now, $\mathbf{A}.\mathbf{X} = [\lambda_1\mathbf{x}_1\ \lambda_2\mathbf{x}_2\ \ldots\ldots\lambda_n\mathbf{x}_n\ ] = \mathbf{X}.\mathbf{\Lambda}$ (1.15)

where $$\mathbf{\Lambda} = \begin{bmatrix} \lambda_1 & 0 & \ldots & 0 \\ 0 & \lambda_2 & \ldots & 0 \\ & & \ldots\ldots & \\ 0 & 0 & \ldots & \lambda_n \end{bmatrix}$$

or, $\mathbf{A} = \mathbf{X}\,\mathbf{\Lambda}\,\mathbf{X}^{-1} = \mathbf{X}\,\mathbf{\Lambda}\mathbf{Y}$ (1.16)

Powerflow equations can be written in matrix form as follows.

$$\begin{bmatrix} \Delta\mathbf{P} \\ \Delta\mathbf{Q} \end{bmatrix} = \begin{bmatrix} J_{p\delta} & J_{pV} \\ J_{q\delta} & J_{qV} \end{bmatrix} \begin{bmatrix} \Delta\boldsymbol{\delta} \\ \Delta\mathbf{V} \end{bmatrix} \tag{1.17}$$

where $\Delta\mathbf{P}$ and $\Delta\mathbf{Q}$ are the changes in the real and reactive powers respectively, $\Delta\boldsymbol{\delta}$ and $\Delta\mathbf{V}$ are the deviations in bus voltage angles and bus voltage magnitudes respectively.

For calculating V-Q sensitivities, one can assume $\Delta\mathbf{P} = 0$

Hence, $\mathbf{J}_{p\delta}.\Delta\boldsymbol{\delta} + \mathbf{J}_{pV}.\Delta\mathbf{V} = 0$
or, $\Delta\boldsymbol{\delta} = -\mathbf{J}_{p\delta}^{-1}.\mathbf{J}_{pV}.\Delta\mathbf{V}$ (1.18)

Now, $\Delta\mathbf{Q} = \mathbf{J}_{q\delta}.\Delta\boldsymbol{\delta} + \mathbf{J}_{qV}.\Delta\mathbf{V} = \mathbf{J}_{q\delta}(-\mathbf{J}_{p\delta}^{-1}.\mathbf{J}_{pV}).\Delta\mathbf{V} + \mathbf{J}_{qV}.\Delta\mathbf{V} = \mathbf{J}_R.\Delta\mathbf{V}$
where, $\mathbf{J}_R = \mathbf{J}_{qV} - \mathbf{J}_{q\delta}.\mathbf{J}_{p\delta}^{-1}.\mathbf{J}_{pV}$

Hence, $\Delta\mathbf{V} = \mathbf{J}_R^{-1}\Delta\mathbf{Q}$ (1.19)

Now, assuming $\mathbf{J}_R = \mathbf{A}$ and using (1.16) one gets, $\mathbf{J}_R = \mathbf{X}\,\mathbf{\Lambda}\mathbf{Y}$
or, $\mathbf{J}_R^{-1} = \mathbf{Y}^{-1}\mathbf{\Lambda}^{-1}\mathbf{X}^{-1} = \mathbf{X}\mathbf{\Lambda}^{-1}\mathbf{Y}$
Using (1.19), $\Delta\mathbf{V} = \mathbf{X}\,\mathbf{\Lambda}^{-1}\mathbf{Y}\,\Delta\mathbf{Q}$

or, $\mathbf{Y}\Delta\mathbf{V} = \mathbf{\Lambda}^{-1}\mathbf{Y}\Delta\mathbf{Q}$;[since, $\mathbf{X}=\mathbf{Y}^{-1}$]

Hence, $\mathbf{v}_m=\mathbf{\Lambda}^{-1}\mathbf{q}_m$

where, $\mathbf{v}_m$ = vector of modal voltage variation

$\mathbf{q}_m$ = vector of modal reactive power variation

Now, $$\Lambda^{-1} = \begin{bmatrix} \lambda_1^{-1} & .....0 \\ 0 & \lambda_2^{-1} ...0 \\ 0 & 0....\lambda_n^{-1} \end{bmatrix}$$

Thus, $\mathbf{v}_{mi} = \lambda_i^{-1}\mathbf{q}_{mi}$, $\forall$ i = 1,…,n

For any i, if $\lambda_i > 0$, then the variation of $\mathbf{v}_{mi}$ and $\mathbf{q}_{mi}$ are in the same direction and the system is voltage stable. When $\lambda_i < 0$ for any i, the system is voltage unstable.

To illustrate the use of the singularity-based voltage stability analysis method, modal analysis is applied on the 10-bus test system [2, 14] shown in Figure 1.6. Data for the 10-bus test system are given in Tables 1.1 to 1.5. Table 1.6 shows the eigenvalues of the reduced Jacobian matrix against load multiplication factor, K. Load multiplication factor is the ratio by which load is increased at 1 pu voltage. Real parts of the eigenvalues are designated as E_1, E_2,…, E_7. Normalized values of the two smallest eigenvalues are plotted against load multiplication factor in Figure 1.7. Computationally obtainable minimum values of eigenvalues correspond to a load multiplication factor of 1.146. An increase in load beyond this load level makes the receiving end voltage unstable. The magnitude of the minimum eigenvalue is therefore used as an indicator of the proximity of an operating point to the point of voltage collapse.

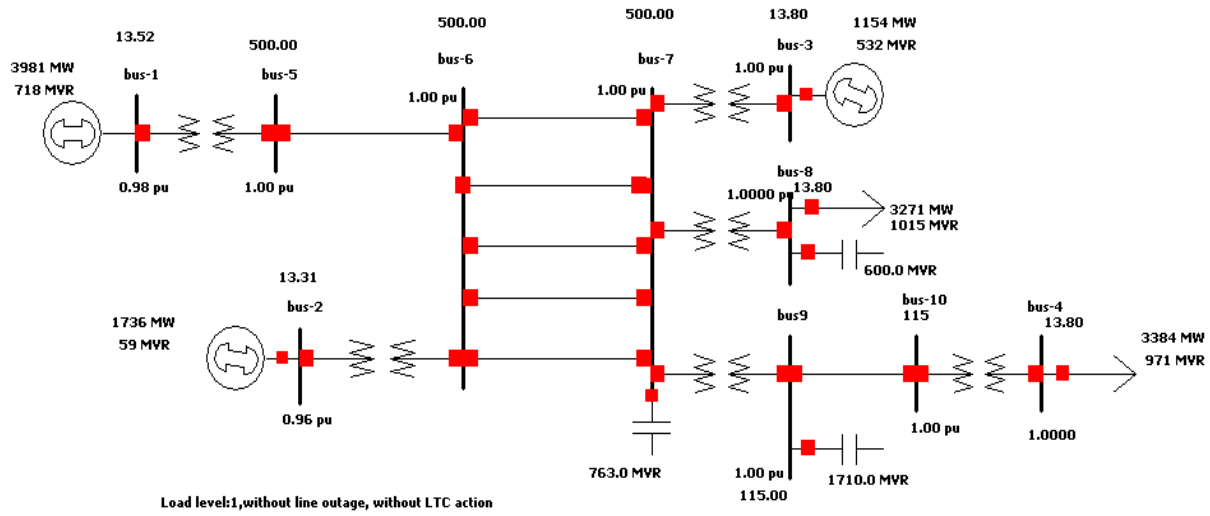

Figure 1.6: Single line diagram of the 10-bus test system

Table 1.1: Transmission lines data (R, X and B in pu on 100MVA base) for the 10-bus test system

End buses	R	X	B
5-6	0.0000	0.0040	0.0000
6-7	0.0015	0.0288	1.1730
9-10	0.0010	0.0030	0.0000

Table 1.2: Transformer data (R, X in pu on 100 MVA base) for the 10-bus test system

End buses	R	X	Ratio
1-5	0.0000	0.0020	0.8857
2-6	0.0000	0.0045	0.8857
3-7	0.0000	0.0125	0.9024
7-8	0.0000	0.0030	1.0664
7-9	0.0000	0.0026	1.0800
10-4	0.0000	0.0010	0.9750

Table 1.3: Shunt capacitor data for the 10-bus test system

Bus	MVAR
7	763
8	600
9	1710

Table 1.4: Base case Load data for the 10-bus test system

Bus	P (MW)	Q (MVAR)
8	3271	1015
4	3384	971

Table 1.5: Base case Generator data for the 10-bus test system

Bus	P (MW)	V (pu)
1	3981	0.9800
2	1736	0.9646
3	1154	1.0400

Table 1.6: Eigenvalues of the reduced Jacobian matrix of the 10-bus test system for different load levels

Load multiplication factor, K	E_1	E_2	E_3	E_4	E_5	E_6	E_7
0.9	2364	1407.1	951.37	26.9	161.27	634.92	390.65
1.0	2203.6	1330.8	425.01	25.062	148.21	598.07	374.9
1.1	2039.5	1253.1	903.38	22.724	134.36	560.11	360.82
1.12	1982.8	1224.6	896.14	21.718	129.64	546.49	356.42
1.14	1885.6	1173.8	881.53	19.795	121.52	522.62	348.03
1.145	1803.7	1129.5	867.34	17.983	114.62	502.09	340.19
1.146	1768.2	1110.4	861.03	17.143	111.59	493.21	336.72

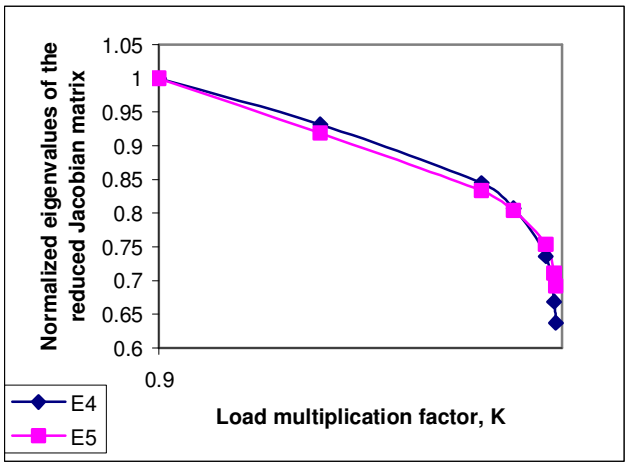

Figure 1.7: Variation of the real parts of the smallest two eigenvalues of the reduced Jacobian matrix against load multiplication factor for the 10-bus test system

4.4 Continuation powerflow

It is numerically difficult to obtain a powerflow solution near the voltage collapse point, since the Jacobian matrix becomes singular. Continuation powerflow is a technique by which the powerflow solutions can be obtained near or at the voltage collapse point [2, 4, 15].

Powerflow equations can be represented as,

$$\mathbf{P}_s = \mathbf{P}(\boldsymbol{\delta},\mathbf{V}) \quad \text{and} \quad \mathbf{Q}_s = \mathbf{Q}(\boldsymbol{\delta},\mathbf{V}) \tag{1.20}$$

where $\mathbf{P}_s$, $\mathbf{Q}_s$ are specified active and reactive powers of busses, δ and $\mathbf{V}$ are bus voltage angles and magnitudes respectively.

Equation (1.20) can be expressed as,

$$\mathbf{f}(\boldsymbol{\delta},\mathbf{V}) = \mathbf{PQ}_{spc} \tag{1.21}$$

where $\mathbf{PQ}_{spc} = [\mathbf{P}_s, \mathbf{Q}_s]^T$.

Considering variation of load as one of the parameters of the power flow equations, (1.21) can be rewritten as,

$$\mathbf{f}(\boldsymbol{\delta},\mathbf{V}) = \mathrm{K}\mathbf{PQ}_{spc} \tag{1.22}$$

where K is the loading parameter. For base case loading, K = 1.

Equation (1.22) can be written as,

$$\mathbf{F}(\boldsymbol{\delta},\mathbf{V},\mathrm{K}) = 0 \tag{1.23}$$

Hence, $$\Delta\mathbf{F} = \frac{\partial\mathbf{F}}{\partial\boldsymbol{\delta}}\Delta\boldsymbol{\delta} + \frac{\partial\mathbf{F}}{\partial\mathbf{V}}\Delta\mathbf{V} + \frac{\partial\mathbf{F}}{\partial\mathrm{K}}\Delta\mathrm{K} \tag{1.24}$$

Now, $\Delta\mathbf{F} = \mathbf{F}(\boldsymbol{\delta}^0,\mathbf{V}^0,K^0) - \mathbf{F}(\boldsymbol{\delta},\mathbf{V},K) = -\mathbf{F}(\boldsymbol{\delta},\mathbf{V},K)$ (1.25)

where $(\boldsymbol{\delta}^0,\mathbf{V}^0,K^0)$ is the solution of (1.23).

Using the above in equation (1.24) and writing in matrix form,

$$\begin{bmatrix} \frac{\partial \mathbf{F}}{\partial \boldsymbol{\delta}} & \frac{\partial \mathbf{F}}{\partial \mathbf{V}} & \frac{\partial \mathbf{F}}{\partial K} \end{bmatrix} \begin{bmatrix} \Delta\boldsymbol{\delta} \\ \Delta\mathbf{V} \\ \Delta K \end{bmatrix} = \left[-\mathbf{F}(\boldsymbol{\delta},\mathbf{V},K)\right] \quad (1.26)$$

This can be written as,

$\mathbf{J} \cdot [\Delta\boldsymbol{\delta}\ \Delta\mathbf{V}\ \Delta K]^T = [-\mathbf{F}(\boldsymbol{\delta},\mathbf{V},K)]$

or, $[\Delta\boldsymbol{\delta}\ \Delta\mathbf{V}\ \Delta K]^T = \mathbf{J}^{-1} \cdot [-\mathbf{F}(\boldsymbol{\delta},\mathbf{V},K)]$ (1.27)

where **J** is the Jacobian matrix.

Near the point of voltage collapse, the Jacobian matrix, **J** approaches singularity; hence it is difficult to calculate $\mathbf{J}^{-1}$ near the collapse point. To overcome the problem one more equation is added assuming one of the variables as fixed. This variable is called the continuation variable.

Assuming that the i^{th} variable is the continuation variable, one can write,

$$[\mathbf{e}_i]\ [\Delta\boldsymbol{\delta}\ \Delta\mathbf{V}\ \Delta K]^T = 0 \quad (1.28)$$

where $[\mathbf{e}_i]$ is the vector having i^{th} element as 1 and all other elements as zero.

Augmenting equation (1.28) to (1.27),

$$\begin{bmatrix} \mathbf{J} \\ \mathbf{e}_i \end{bmatrix} \left[\Delta\boldsymbol{\delta}\ \Delta\mathbf{V}\ \Delta K\right]^T = \begin{bmatrix} -\mathbf{F}(\boldsymbol{\delta},\mathbf{V},K) \\ 0 \end{bmatrix} \quad (1.29)$$

The difference vector $[\Delta\boldsymbol{\delta}\ \Delta\mathbf{V}\ \Delta K]^T$ is found from (1.29) and added with the initial assumption of vector $[\boldsymbol{\delta},\mathbf{V},K]$ to get the predictor.

The predictor may not be exactly on the desired solution curve. To get the exact solution, the following corrector equations are added with the set of equations (1.23).

$x_i = \mu$ or $x_i - \mu = 0$

where μ is the assumed fixed value of the continuation variable.

Thus the system of equations becomes,

$\mathbf{F}(\boldsymbol{\delta},\mathbf{V},K) = 0$, and, $x_i - \mu = 0$

In the above set of equations, the number of variables is equal to the number of equations. Thus it can be solved by the Newton-Raphson method, having the predictor as the initial guess.

Continuation power flow allows the load voltage to be computed even when the power flow Jacobian matrix is singular. The complete PV curve, including the nose point and the lower part of the

curve, can be drawn using continuation power flow. Figure 1.8 shows the complete PV curve of bus-4 for the 10-bus test system, using PSAT [16] that uses continuation power flow.

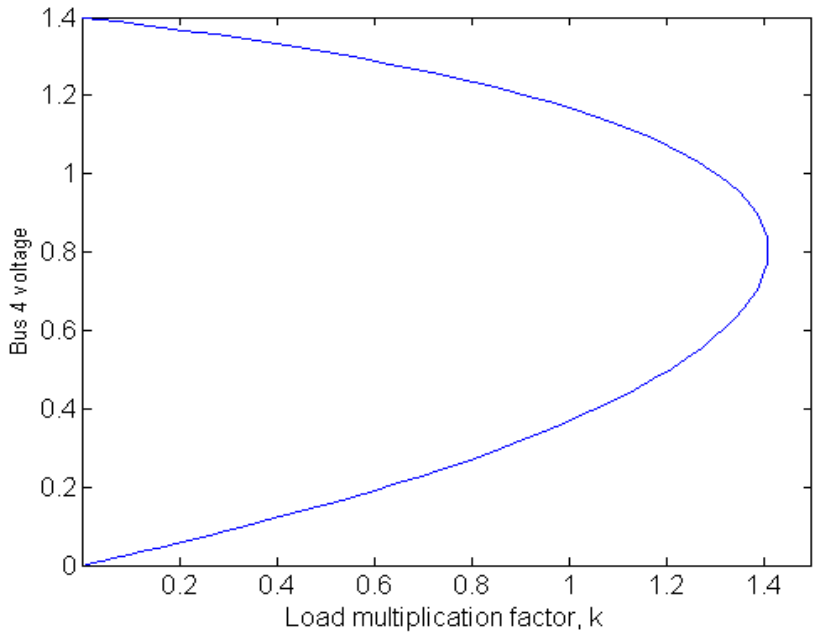

Figure 1.8: PV curve of bus-4 for the 10-bus test system, obtained by using continuation power flow

5. Detailed voltage stability analysis of the 10-bus test system for different loading conditions

Voltage stability analysis is carried out for the 10-bus test system described earlier in this chapter. Different transformer tap settings for different load levels and corresponding generations for the 10-bus test system are given in Tables 1.7 to 1.9 [2, 17]. Simulations are carried out with and without load tap changers (LTCs) between bus 4 and bus 10. The effect of line outage on voltage stability is also studied.

Simulations are done in PowerWorld Simulator [18]. Base case conditions for three load levels are as follows.

- All the transformers are at fixed tap [Table 1.7].
- The load at bus 8 [Table 1.8] is of constant power type, while that of bus 4 is 50% constant power and 50% constant current.

Simulation results are recorded at four different operating conditions (or 'snapshots') at three different load levels and are presented in Tables 1.10 to 1.12. The effect of LTC between bus 10 and 4 on voltages at different busses, as well as the reactive power generation and consumption in nearby busses are studied.

At 'snapshot 1', i.e., when there is no line outage in the system and the LTC is kept at fixed tap position, bus 4 voltage reduces with increased loading. At load level 3, the voltage level is very low and it needs LTC operation to restore the voltage.

When the LTC is turned on, there is a considerable increase in load bus (bus 4) voltage. With higher voltage, load power consumption increases (because of 50% constant current load), which leads to the reduction of voltages in the adjacent busses. At reduced voltage, output of the shunt capacitor reduces, thereby stressing the generators to produce more reactive power.

With outage of one line between bus 6 and bus 7, less power is available to the load from the two generators at the other end of the system, thus the voltages reduce at the load end busses. Output of the shunt capacitor falls because of reduced voltage and as a result load voltage deceases further. Generators are more stressed and produce more reactive power to compensate for the loss.

Even with operation of LTC after line outage, load voltage is not restored significantly. A reason for this is the shortage of available reactive power at the load end because of the line outage and reduced efficiency of capacitors due to reduced voltage. In an attempt to raise the voltage, LTC increases load power consumption. If the load is slightly increased, it can be seen that this reduces the voltage further and eventually the system faces a voltage collapse.

Modal analysis was carried out on the reduced Jacobian matrix of the system for different operating conditions and the results are shown in Table 1.13. It can be seen that the minimum eigenvalue of the reduced Jacobian matrix reduces with load. It can be used as an indicator of the closeness of the operating point to the point of voltage collapse.

Table 1.7: Transformer data for different load levels for the 10-bus test system
(R, X in pu on 100 MVA base)

End busses	R	X	Tap setting
10-4	0.0000	0.0010	0.9750 (load level: 1) 0.9938 (load level: 2) 1.0000 (load level: 3)

Table 1.8: Load data for different load levels for the 10-bus test system

Bus	P (MW)	Q (MVAR)	Load level
8	3271 3320 3335	1015 1030 1035	1 2 3
4	3384 3435 3460	971 985 993	1 2 3

Table 1.9: Generator data for different load levels for the 10-bus test system

Bus	P (MW)	V (pu)	Load level
1	3981 4094 4252	0.9800 0.9800 0.9800	1 2 3
2	1736 1736 1736	0.9646 0.9646 0.9646	1 2 3
3	1154 1154 1154	1.0400 1.0400 1.0400	1 2 3

Table 1.10: Load voltages and reactive power outputs of generator 2 and 3 at load level 1

Contingency	V4	V8	V7	QG3 (MVAR)	QG2 (MVAR)
Without outage, fixed tap	0.98	1.03	1.11	390	-94
Without outage, LTC active	1.00	1.01	1.10	505	31
Line outage, fixed tap	0.95	0.96	1.05	700	440
Line outage, LTC active	0.93	0.92	1.00	700	723

Table 1.11: Load voltages and reactive power outputs of generator 2 and 3 at load level 2

Contingency	V4	V8	V7	QG3 (MVAR)	QG2 (MVAR)
Without outage, fixed tap	0.96	1.03	1.11	390	-93
Without outage, LTC active	0.99	0.99	1.08	627	164
Line outage, fixed tap	0.91	0.91	1.00	700	724
Line outage, LTC active	0.92	1.01	1.09	543	146

Table 1.12: Load voltages and reactive power outputs of generator 2 and 3 at load level 3

Contingency	V4	V8	V7	QG3 (MVAR)	QG2 (MVAR)
Without outage, fixed tap	0.95	1.02	1.11	401	-81
Without outage, LTC active	0.99	0.98	1.07	700	249

Table 1.13: Eigenvalues of the reduced Jacobian matrix for different contingencies and load levels for the 10-bus test system

	Without outage, fixed tap	Without outage, LTC active	Line outage, fixed tap	Line outage, LTC active
Load level 1	2203.6	2272.3	2190.9	2249.1
	1330.8	1313.1	1230.3	1206.2
	925.01	919.68	899.14	893.12
	25.062	24.737	21.788	21.376
	148.21	143.97	135.57	130.19
	598.07	588.45	560.6	547.69
	374.9	371.46	347.46	343.47
Load level 2	2151.1	2284.1	2191.8	2219.2
	1329.8	1293.5	1206.4	1193.5
	924.85	913.89	893.15	889.96
	24.979	24.308	21.228	21.002
	148.54	139.86	130.69	127.86
	598.04	578.28	548.21	541.37
	374.75	367.68	343.41	341.31
Load level 3	2130.8	2294.4	2194.9	2203.7
	1327.8	1281.2	1191.4	1187
	924.32	910.3	889.43	888.33
	24.903	24.043	20.877	20.797
	148.34	137.29	127.63	126.66
	597.18	571.89	540.44	538.08
	374.38	365.35	340.92	340.2

References

[1] C. W. Taylor, *Power System Voltage Stability*, McGraw-Hill, 1994.

[2] P. Kundur, *Power System Stability and Control*, McGraw-Hill, 1993.

[3] IEEE/CIGRE Joint Task Force on Stability Terms and Definitions, "Definition and Classification of Power System Stability", *IEEE Transactions on Power Systems*, Vol. 5, No. 2, May 2004, pp. 1387–1401.

[4] T. V. Cutsem, C. Vournas, *Voltage Stability of Electric Power Systems*, Kluwer Academic Publishers, 1998.

[5] IEEE/PES Power System Stability Subcommittee Special Publication, *Voltage Stability Assessment, Procedures and Guides*, Final Draft, January 1999.

[6] S. C. Savulescu, *Real-time Stability in Power Systems*, Springer, 2006.

[7] J. Machowski, J. W. Bialek, J. R. Bumby, *Power System Dynamics and Stability*, John Wiley & Sons, 1997.

[8] J. A. Diaz de Leon II, C. W. Taylor, "Understanding and Solving Short-Term Voltage Stability Problems', *IEEE Power Engineering Society Summer Meeting*, 2002, pp. 745-752.

[9] I. Dobson, "Observations on the Geometry of Saddle Bifurcation and Voltage Collapse in Electrical Power Systems", *IEEE Transactions on Circuits and Systems*, Vol. 39, No. 3, March 1992, pp. 240-243.

[10] H. D. Chiang, I. Dobson, R. Thomas, J.S. Thorp, L. F. Ahmed, "On Voltage Collapse in Electric Power Systems", *IEEE Transactions on Power Systems*, Vol. 5, No. 2, May 1990, pp.601–611.

[11] F. Dong, B. H. Chowdhury, M. Crow, L. Acar, "Cause and Effects of Voltage Collapse-Case Studies with Dynamic Simulations", *IEEE Power Engineering Society General Meeting*, 2004, pp. 1806-1812.

[12] I. Dobson, "The Irrelevance of Load Dynamics for the Loading Margin to Voltage Collapse and Its Sensitivities", *Bulk Power System Voltage Phenomena-III, Voltage Stability, Security and Control*, Davos, Switzerland, August, 1994.

[13] I. Dobson, "Towards a Theory of Voltage Collapse in Electric Power Systems", *Systems and Control Letters* 13, 1989, pp. 253-262.

[14] B. Gao, G.K. Morison, and P. Kundur, "Voltage stability evaluation using modal analysis," *IEEE Transactions on Power Systems*, Vol. 7, No. 4, November 1992, pp.1529–1542.

[15] R. Seydel, *From Equilibrium to Chaos*, Elsevier, New York, 1988.

[16] F. Milano, "An Open Source Power System Analysis Toolbox," *IEEE Transactions on Power Systems*, Vol. 20, No. 3, August 2005, pp.1199–1206.

[17] G. K. Morison, B. Gao and P. Kundur, "Voltage stability analysis using static and dynamic approaches", *IEEE Transactions on Power Systems*, Vol. 8, No. 3, August 1993, pp. 1159–1171.

[18] PowerWorld Simulator, Version 10.0 SCOPF, PVQV, PowerWorld Corporation, Champaign, IL 61820, 2005.